chemistry proceedings

MDPI

Proceeding Paper

Computational Study of P, S and Se Analogues of Naphthalenediimide as Cathode Components in Batteries

M. Pilar Vázquez-Tato [1], Francisco Meijide [2], José Vázquez Tato [2] and Julio A. Seijas [1,*]

[1] Departamento de Química Orgánica, Facultade de Ciencias, Universidade de Santiago de Compostela, Campus Terra, 27080 Lugo, Spain; e-mail@e-mail.com
[2] Departamento de Química Física, Facultade de Ciencias, Universidade de Santiago de Compostela, Campus Terra, 27080 Lugo, Spain; e-mail@e-mail.com (F.M.); e-mail@e-mail.com (J.V.T.)
* Correspondence: julioa.seijas@usc.es

Abstract: Several computational studies have been published to predict the behaviour of naphthalenediimides (NDI) in the transport of electrons in batteries, as well as their physical properties. This communication compares NDI with their analogues resulting from replacing the nitrogen atom by phosphorus, sulphur, or selenium. The calculations were performed with Gaussian 16 using the theory level B3LYP/6-311++g(d,p) in gas and in DMSO, which allows obtaining the values for IP, EA, HOMO, LUMO, Fukui indices, redox potential, and reorganization free energies.
The results achieved indicate that the analogues studied could be an interesting alternative to naphthalenediimides, and that their experimental study may be new tools for lithium batteries.

Keywords: keyword 1; keyword 2; keyword 3 (List three to ten pertinent keywords specific to the article yet reasonably common within the subject discipline.)

Citation: Vázquez-Tato, P.; Meijide, F.; Tato, J.V.; Seijas, J.A. Computational Study of P, S and Se Analogues of Naphthalenediimide as Cathode Components in Batteries. **2021**, *3*, x. https://doi.org/10.3390/xxxxx

Academic Editor: Julio A. Seijas

Published: 15 November 2021

1. Introduction

Electrochemical energy storage (EES) devices such as lithium or more recently sodium-ion batteries (LIB, SIB) represent one of the most promising approaches to enable the widespread utilization of renewable energy sources [1,2]. One of the biggest questions about LIB and SIB electrodes is the design of new cathode materials with high capacity, high voltage, long-term stability, and low molecular weight. An extensive literature gathers results of the studies, both theoretical and experimental, of the use of derivatives of naphthalenediimides (NDI) as materials for cathodes [3]. This series of molecules present ionic interactions during the reduction processes between the radical anion/dianion and metal cations, the possibility of shifting the formal potential by making changes in the molecule, and their reversible redox chemistry.

However, little to no studies have been carried out on condensed structures derived from 1,4,5,8 tetracarboxylic acid, in which the nitrogen in the NDI, are changed by phosphorus, sulphur or selenium, probably due to its greater difficulty when preparing them. However, some reports on mellitic anhydride derivatives discovered that the replacement of nitrogen with a phosphorus atom led to the increase in the reduction potential, showing the phosphorus-containing organic materials as promising alternatives for well-known bisimide organic electron-acceptor materials, since they may exhibit even lower LUMO levels than those of bisimides [4]. This would allow the design of new stable electron acceptors or ambipolar materials for organic electronics application.

2. Results and Discussion

As model compounds for the study, the following compounds were chosen: 2,7-dimethylbenzo[*lmn*][3,8]phenanthroline-1,3,6,8(2H,7H)-tetraone (**1**), 2,7-dimethylisophosphinolino[6,5,4-*def*]isophosphinoline-1,3,6,8(2H,7H)-tetraone (**2**),

isothiochromeno[6,5,4-def]isothiochromene-1,3,6,8-tetraone (**3**), and isoselenochromeno[6,5,4-def]isoselenochromene-1,3,6,8-tetraone (**4**) (Figure 1).

In the case of **1** and **2**, the positions 2 and 7 of the pyrene-1,3,6,8(2H,7H)-tetraone skeleton were occupied by N-Me and P-Me, to avoid the issue of the anion on Nitrogen or Phosphorous atom, respectively, if the N-H or P-H were used [5].

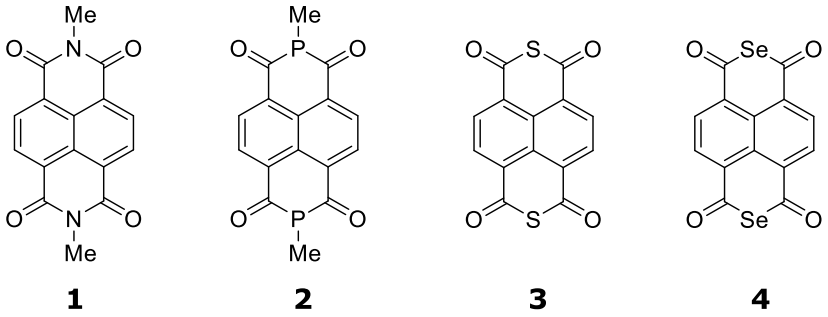

Figure 1. Compounds studied.

The process can be generalized as the enolization and its reverse process in the carbonyl group, which can be promoted by a conjugated structure, either aromatic or aliphatic [3]. When a compound is used as the cathode material for rechargeable lithium batteries, its reduction and oxidation are accompanied by the association and disassociation of Li^+ ions with oxygen. Ideally, each formula unit is able to transfer up to four electrons through four consecutive steps (Scheme 1).

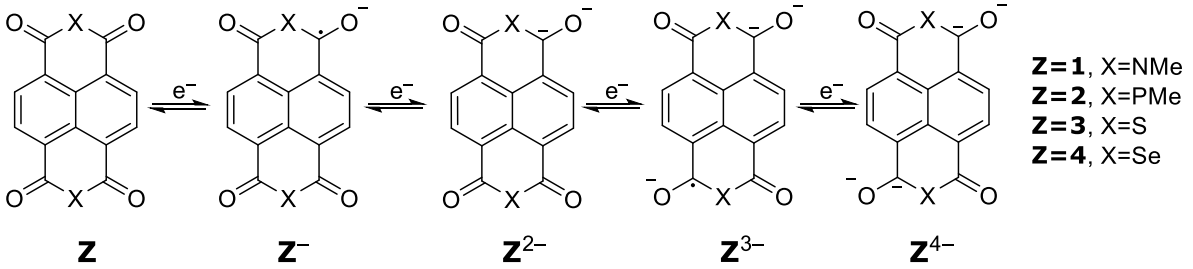

Scheme 1. Electron transfer in reduction.

Electron transfer during an electrochemical process leads to the redox of the compound. The redox ability of the compound can be quantitatively described by the redox potential. The performance of organic electrical devices is highly dependent on the oxidation potential (E_{OX}) and the reduction potential (E_{RED}) of the used materials. These potentials for the materials govern their capability to capture (or inject) holes and electrons, respectively, in the devices.

The thermodynamic cycle for the Gibbs free energy of the oxidation and reduction reaction of the molecule A is displayed in Scheme 2 [6].

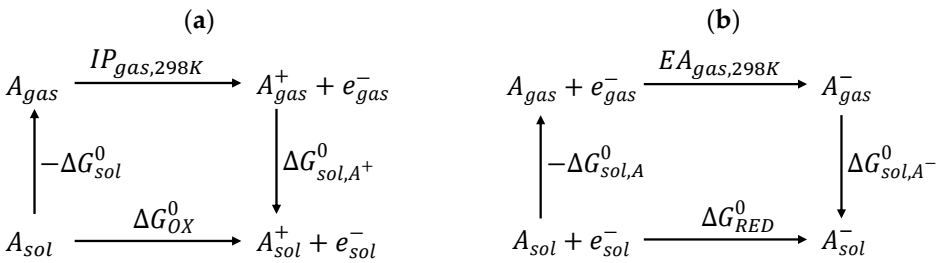

Scheme 2. Thermodynamic cycle for the Gibbs free energy.

The ΔG_{sol} is evaluated as the electronic energy difference of the molecule in the gas phase and the solvated one using the equilibrium geometry obtained in vacuum.

Marcus theory was used to estimate the charge transfer properties. According to this theory, the reorganization energy (λ) has both intra- and intermolecular contributions. The former reflects the deformation of molecular geometry in order to accommodate charge transfer; and the latter reflects the electronic polarization of the surrounding molecules, being much smaller than the intramolecular one and is usually neglected. The intramolecular reorganization energy can be evaluated either from the adiabatic potential-energy surfaces or from normal-mode analysis [7]. In this method, the hole and electron reorganization energies ($\lambda_{h/e}$) are defined by the following equation:

$$\lambda_{h/e} = \lambda^1 + \lambda^2$$

$$\lambda^1 = E_N(Q_{h/e}) - E_N(Q_N)$$

$$\lambda^2 = E_{h/e}(Q_N) - E_{h/e}(Q_{h/e})$$

where, $E_N(Q_N)$ and $E_{h/e}(Q_{h/e})$ are the ground-state energies of the optimized neutral and ionic states, respectively, $E_N(Q_{h/e})$ is the energy of the charged molecules at the optimal geometry of the neutral molecules, and $E_{h/e}(Q_N)$ is the energy of the neutral molecules at the optimal ionic geometry.

The adiabatic ionization potential $IP_{(a)}$ and adiabatic electron affinity $EA_{(a)}$ are two important parameters to evaluate the oxidation and reduction ability of charged organic molecules. Especially, the large $EA_{(a)}$ is beneficial for stabilizing the organic radical anions. Meanwhile, the large $EA_{(a)}$ decreases the electron injection energy barrier and hence is helpful for electron transport [8]. Thus, the corresponding adiabatic IPs and EAs were obtained with following equations:

$$IP_{(a)} = E_h(Q_h) - E_N(Q_N)$$

$$EA_{(a)} = E_N(Q_N) - E_e(Q_e)$$

All these calculations were carried out with Gaussian16 at B3LYP/6311g++(d,p) level [9]. Dimethylsulfoxide (DMSO) was chosen (using a polarizable continuum model) for the solution calculations, due to its low toxicity and it is a non-hazardous solvent that can solubilize a vast variety of organic compounds [10]. The vibrational frequency analysis was performed at the same level of theory and the resulted positive frequencies confirmed that the optimized geometries were found at the real minima on the potential energy surfaces.

The molecular structure of designed molecules in their ground state was fully optimized and their optimized geometries rendered the energy and shape of their LUMO and HOMO. This was carried out for each of the species involved in the four steps of the electronic transference between the neutral state and the $4-$ anion. The energy of the frontier molecular orbitals of organic materials is one of the key factors in influencing the charge transport properties and the intrinsic air-stability of the materials. The energy gap (E_g) for the five states of the compounds follows the order $E_{gN} > E_{g2-} > E_{g-} > E_{g3-} > E_{g4-}$, the higher values being for the neutral species (Figure 2).

Molecular electrostatic potential surfaces enable to visualize the charge distributions and the charge related properties of the molecules. Electronic total density and electrostatic cube files were generated for each species and Gabedit 2.5.1 [11] was used to create the electrostatic potential mapped on the electronic density surface graphics are shown in Table 1. The colour code is between −0.4 and 0.1 eV for all examples. Carbonyl oxygens are the most negative areas in the surfaces.

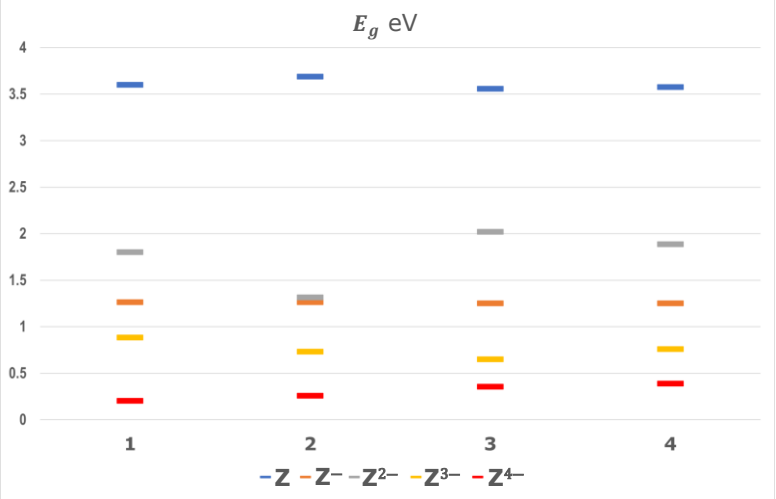

Figure 2. Energy gap between HOMO and LUMO orbital.

Table 1. MEP surfaces for the compounds studied.

Charge	1	2	3	4
0				
1–				
2–				
3–				
4–				
	–0.4			0.1

The redox potentials for $[\mathbf{Z}]^{0/-}$, $[\mathbf{Z}]^{0/2-}$, $[\mathbf{Z}]^{0/3-}$, $[\mathbf{Z}]^{0/4-}$ (Scheme 3) were calculated as mentioned above, together with the corresponding electron reorganization energies (λ) to

check the feasibility of the reduction process. Lower λ values are related to higher charge carrier mobility.

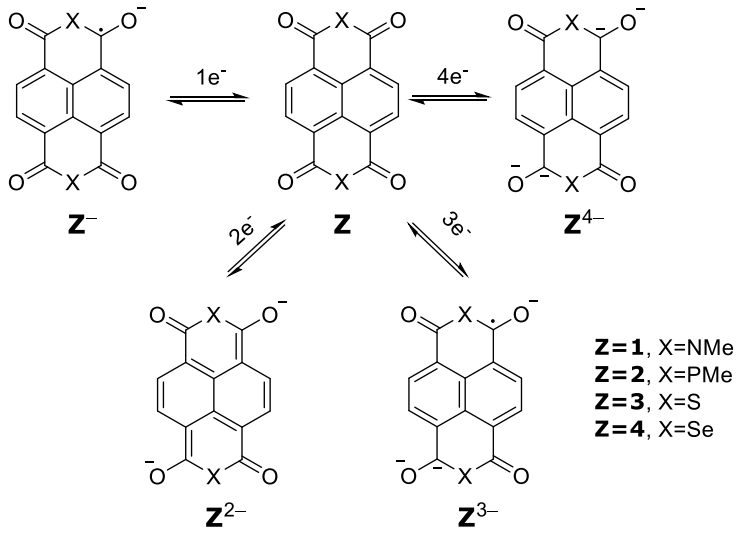

Scheme 3.

The reduction potentials (Table 2) were higher with the increase in the number of electrons transferred, being for compounds **4** and **3** the larger ones. It is noteworthy that $[\mathbf{1}]^{0/-} > [\mathbf{2}]^{0/-}$ and $[\mathbf{1}]^{0/2-} > [\mathbf{2}]^{0/2-}$ but $[\mathbf{1}]^{0/3-} < [\mathbf{2}]^{0/3-}$ and $[\mathbf{1}]^{0/4-} < [\mathbf{2}]^{0/4-}$.The electron reorganization energies show the higher value for the phosphorous compound, except for $\mathbf{2}\lambda_{0/3-}$.

Table 2.

Compound	1	2	3	4
$[\mathbf{Z}]^{0/-}$	−3.96	−3.88	−4.28	−4.24
$[\mathbf{Z}]^{0/2-}$	−7.20	−7.14	−7.84	−7.78
$[\mathbf{Z}]^{0/3-}$	−8.41	−9.58	−10.11	−10.12
$[\mathbf{Z}]^{0/4-}$	−9.08	−11.51	−11.47	−11.74
$\lambda_{0/-}$	0.35	0.48	0.34	0.35
$\lambda_{0/2-}$	1.33	1.76	1.28	1.31
$\lambda_{0/3-}$	1.25	1.80	1.83	1.94
$\lambda_{0/4-}$	1.23	2.01	1.58	1.70

Reduction potentials for species $[\mathbf{Z}]^{0/-}$, $[\mathbf{Z}^{\cdot-}]^{-/2-}$, $[\mathbf{Z}^{2-}]^{2-/3-}$, $[\mathbf{Z}^{3-}]^{3-/4-}$ (Scheme 1), and their respective λ values were calculated, in order to detect any anomalous value which would evidence a special difficulty in the charge carrier mobility (Table 3).

Table 3.

Compound	1	2	3	4
$[\mathbf{Z}]^{0/-}$	−3.96	−3.88	−4.28	−4.24
$[\mathbf{Z}^{-}]^{-/2-}$	−3.26	−3.26	−3.60	−3.55
$[\mathbf{Z}^{2-}]^{2-/3-}$	−1.23	−2.44	−2.28	−2.34
$[\mathbf{Z}^{3-}]^{3-/4-}$	−0.68	−1.93	−1.37	−1.62
$\lambda_{0/-}$	0.35	0.48	0.34	0.35
$\lambda_{-/2-}$	0.32	0.40	0.31	0.31
$\lambda_{2-/3-}$	0.04	0.03	0.36	0.30
$\lambda_{3-/4-}$	0.01	0.06	0.11	0.28

This approach to the evaluation of the reduction potentials turned out to be similar to the ones in Table 2, with the potentials of the transfer of **1**, **2**, **3** and **4** electrons like the sum of the individual transfer.

Moreover, similar values are obtained for the reduction potentials of the compounds $[\mathbf{Z}]^{0/4-}$, both considering the joint transfer of the four electrons and the sum of the rearrangement energies of the four consecutive transfer processes of a single electron (Table 4).

Table 4.

	$[\mathbf{1}]^{0/4-}$	$[\mathbf{2}]^{0/4-}$	$[\mathbf{3}]^{0/4-}$	$[\mathbf{4}]^{0/4-}$
$[\mathbf{Z}]^{0/-} + [\mathbf{Z}^{-}]^{-/2-} + [\mathbf{Z}^{2-}]^{2-/3-} + [\mathbf{Z}^{3-}]^{3-/4-}$	−9.12	−11.51	−11.53	−11.74
$[\mathbf{Z}]^{0/4-}$	−9.08	−11.51	−11.47	−11.74

In evaluating electron rearrangement energy, the two alternatives are that either the transfer occurs with the motion of one electron, or it occurs simultaneously with several electrons at the same time [12]. The adiabatic potential energy surface method, which is used for calculating the reorganization energy, is described in Figure 3 for dianion for both different cases: through the monoanion with transfer of one electron in two stages and when two electrons are transferred in a single process.

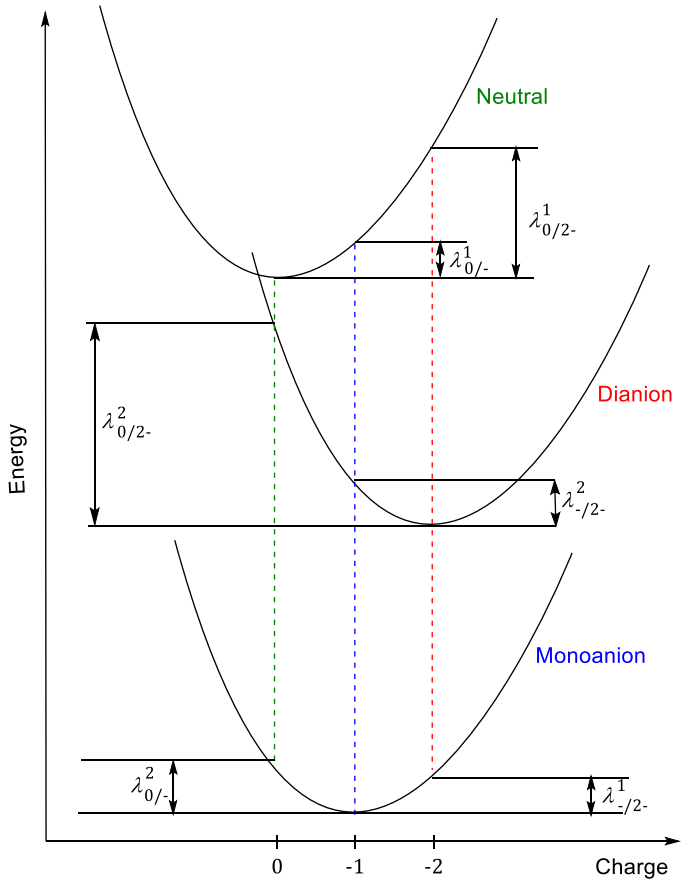

Figure 3. Schematic plot of reorganization energy for electron transfer for compounds **1**, **2**, **3** and **4**.

Unlike the values of the reduction potentials, the lambda values turned out to be non-additive when calculated for the consecutive additions of the electrons to successively obtain the mono, di, tri and tetra anions. Thus, the values for $\lambda_{0/2-}$, $\lambda_{0/3-}$, $\lambda_{0/4-}$ for simultaneous transfers are greater than those calculated from the sum of each one electron transfer (Figure 4, Table 5):

$$\lambda^{\Sigma}_{0/2-} = \lambda_{0/-} + \lambda_{-/2-}$$

$$\lambda^{\Sigma}_{0/3-} = \lambda_{0/-} + \lambda_{-/2-} + \lambda_{-/3-}$$

$$\lambda^{\Sigma}_{0/4-} = \lambda_{0/-} + \lambda_{-/2-} + \lambda_{2-/3-} + \lambda_{3-/4-}$$

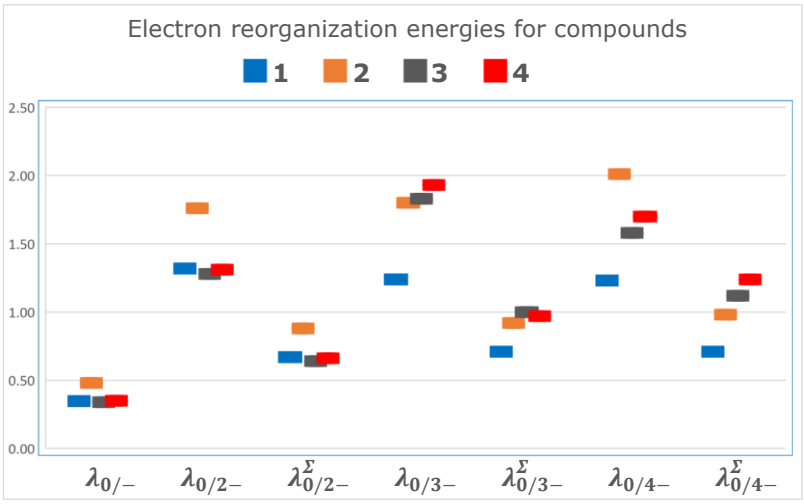

Figure 4.

Table 5. Comparative values for reorganization energy of electrons.

Compound	1	2	3	4
$\lambda_{0/2-}$	1.32	1.76	1.28	1.31
$\lambda^{\Sigma}_{0/2-}$	0.67	0.88	0.64	0.66
$\lambda_{0/3-}$	1.24	1.80	1.83	1.93
$\lambda^{\Sigma}_{0/3-}$	0.71	0.92	1.00	0.97
$\lambda_{0/4-}$	1.23	2.01	1.58	1.70
$\lambda^{\Sigma}_{0/4-}$	0.71	0.98	1.12	1.24

The Frank-Condon principle, as applied in the framework of the Marcus theory for charge transfer, provides another via to the evaluation of reorganization energies [13]. Therefore, for an anion of valence n:

$$\lambda_{0/n} = n^2 \lambda_{0/-}$$

Thus, in case of $\lambda_{0/-} = 1.0\ eV$, reorganization energy for simultaneous two- and three-electron transfer would be $4.0\ eV$ and $9.0\ eV$, respectively (Table 6). These values differ from the ones calculated previously and therefore considered as approximations far from real values.

Table 6.

Compound	1	2	3	4
$\lambda_{0/-}$ ($\mathbf{Z}\rightarrow\mathbf{Z}^{-}$)	0.35	0.48	0.34	0.35
$4\lambda_{0/-}$ ($\mathbf{Z}\rightarrow\mathbf{Z}^{2-}$)	1.38	1.92	1.35	1.40
$9\lambda_{0/-}$ ($\mathbf{Z}\rightarrow\mathbf{Z}^{3-}$)	3.12	4.31	3.05	3.15
$16\lambda_{0/-}$ ($\mathbf{Z}\rightarrow\mathbf{Z}^{4-}$)	5.54	7.67	5.41	5.61

Gabedit 2.5.1 software allowed to determine the Fukui indices. These were calculated using the frontier orbitals of the **Z** compounds as neutral, mono-, di-, tri- and tetra-anions

(Table 7). These values are represented in Figure 5 to facilitate the comparison of the four compounds studied for each type of anion.

The values of the descriptors of the Fukui indices for the neutral compounds (**Z**) show only small differences. The differences increase for the mono anionic compounds, establishing similarity on the one hand between $\mathbf{1}^-$ and $\mathbf{2}^-$ and on the other between $\mathbf{3}^-$ and $\mathbf{4}^-$. The dianions $\mathbf{Z}^{2-}$ show values inside the order of magnitude of **Z** and $\mathbf{Z}^-$. In the case of $\mathbf{Z}^{3-}$ and $\mathbf{Z}^{4-}$ the indices: ω (Electrophilicity index), ω–(propensity to donate electron), ω+ (propensity to accept electron), Qmax (Maximal electronic charge accepted by an electrophile), Demin (Energy decrease if the electrophile take Qmax) show values of a larger order of magnitude that led to think that is due to a defect in the concept, rather than a trustable prediction.

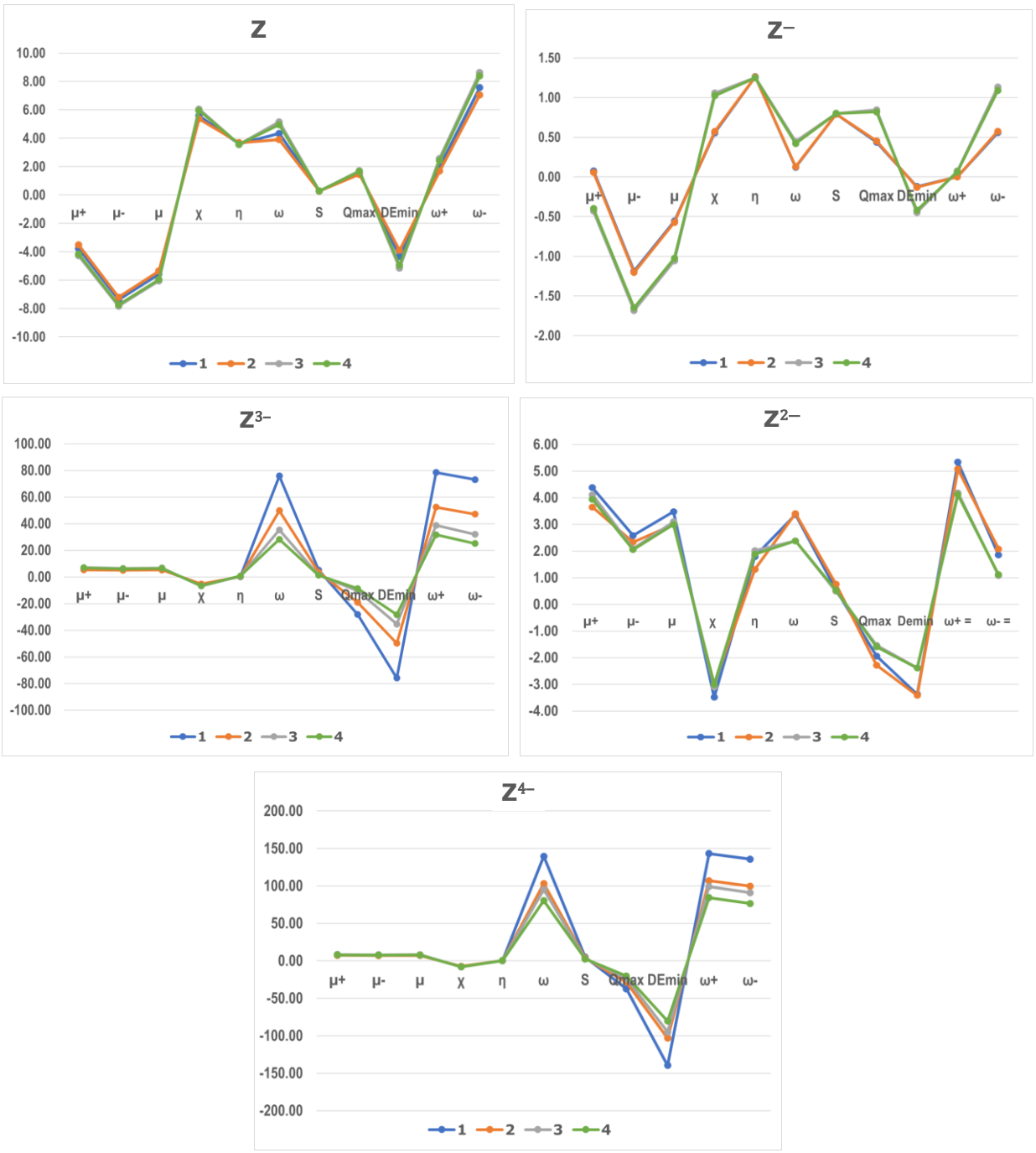

Figure 5. Graphic representation of Fukui indices for the compounds studied.

Table 7. μ+ = eLUMO, μ − = eHOMO, μ = Chemical potential = $(\mu + + \mu -)/2$, η = Chemical hardness = $(\mu + -\mu -)$, χ = Electronegativity = $-\mu$, ω = Electrophilicity index = $\mu^2/(2\eta)$, ω − = propensity to donate electron = $\mu -^2/(2\eta)$, ω+ = propensity to accept electron = $\mu+^2/(2\eta)$, S = Global softness = $1/\eta$, Qmax = Maximal electronic charge accepted by an electrophile = $-\mu/\eta$, Demin = Energy decrease if the electrophile take Qmax = $-\mu^2/(2\eta)$. All values correspond to eV.

Compound	**1**	**2**	**3**	**4**
μ+	−3.78	−3.52	−4.28	−4.17
μ −	−7.38	−7.21	−7.83	−7.74
μ	−5.58	−5.36	−6.05	−5.95
χ	5.58	5.36	6.05	5.95
η	3.60	3.69	3.56	3.58
ω	4.33	3.90	5.15	4.96
S	0.28	0.27	0.28	0.28
Qmax	1.55	1.45	1.70	1.67
DEmin	−4.33	−3.90	−5.15	−4.96
ω+	1.99	1.68	2.57	2.43
ω −	7.57	7.04	8.62	8.38
Compound	**1^-**	**2^-**	**3^-**	**4^-**
μ+	0.08	0.06	−0.43	−0.40
μ −	−1.19	−1.20	−1.68	−1.65
μ	−0.56	−0.57	−1.06	−1.02
χ	0.56	0.57	1.06	1.02
η	1.26	1.26	1.25	1.25
ω	0.12	0.13	0.45	0.42
S	0.79	0.79	0.80	0.80
Qmax	0.44	0.45	0.85	0.82
DEmin	−0.12	−0.13	−0.45	−0.42
ω+	0.00	0.00	0.07	0.06
ω −	0.56	0.57	1.13	1.09
Compound	**1^{2-}**	**2^{2-}**	**3^{2-}**	**4^{2-}**
μ+	4.38	3.65	4.11	3.94
μ −	2.58	2.34	2.09	2.06
μ	3.48	3.00	3.10	3.00
χ	−3.48	−3.00	−3.10	−3.00
η	1.80	1.32	2.02	1.89
ω	3.37	3.41	2.38	2.38
S	0.56	0.76	0.50	0.53
Qmax	−1.94	−2.28	−1.54	−1.59
DEmin	−3.37	−3.41	−2.38	−2.38
ω+	5.34	5.08	4.19	4.12
ω −	1.85	2.08	1.08	1.12
Compound	**1^{3-}**	**2^{3-}**	**3^{3-}**	**4^{3-}**
μ+	5.48	5.34	7.09	6.93
μ −	5.29	5.07	6.44	6.18
μ	5.38	5.20	6.77	6.55
χ	−5.38	−5.20	−6.77	−6.55
η	0.19	0.27	0.65	0.76
ω	75.81	49.75	35.31	28.32
S	5.23	3.68	1.54	1.32
Qmax	−28.16	−19.12	−10.43	−8.64
DEmin	−75.81	−49.75	−35.31	−28.32

ω+	78.52	52.39	38.77	31.69
ω −	73.14	47.19	32.00	25.14
Compound	**1^{4-}**	**2^{4-}**	**3^{4-}**	**4^{4-}**
μ+	7.57	7.39	8.37	8.09
μ −	7.37	7.14	8.02	7.70
μ	7.47	7.26	8.20	7.90
χ	−7.47	−7.26	−8.20	−7.90
η	0.20	0.26	0.35	0.39
ω	139.47	103.20	95.02	80.33
S	4.99	3.91	2.83	2.58
Qmax	−37.32	−28.41	−23.18	−20.35
DEmin	−139.47	−103.20	−95.02	−80.33
ω+	143.23	106.87	99.16	84.32
ω −	135.75	99.60	90.96	76.43

3. Conclusions

In summary, three model compounds analogous of 1,4,5,8-naphthalene diimides (NDI) resulting from substituting N by P, S and Se atoms have been studied. The resultant compounds: **1**, **2**, **3** and **4** have been analysed theoretically (DFT B3LYP/6311g++(d,p) with Gaussian16) in order to check their properties and their use as alternatives to NDI in the multiple applications that they present in electron and energy transfer processes. The reduction potentials have been calculated for **Z**, $\mathbf{Z}^{-}$, $\mathbf{Z}^{2-}$, $\mathbf{Z}^{3-}$, obtaining values that indicate, especially for the first reduction process, that both the case of S (**3**) and the case of Se (**4**) could be of interest as alternatives for NDI. This constitutes a preliminary communication, which motivates the need for more extensive studies including the comparison with different functionalities, and both the calculation and evaluation of the influence that the substituents can have on the properties, as well as addressing the laboratory synthesis of the compounds **3** and **4**, whose skeletons have not been synthesized yet.

Acknowledgments: The authors thank the Ministerio de Ciencia y Tecnología (Project MAT2017-86109P) for the financial support. Centro de Supercomputación de Galicia (CESGA, https://www.cesga.es/) is acknowledged for the computing facilities with G16.

References

1. Hernández-Burgos, K.; Burkhardt, S.E.; Rodríguez-Calero, G.G.; Hennig, R.G.; Abruña, H.D. Theoretical Studies of Carbonyl-Based Organic Molecules for Energy Storage Applications: The Heteroatom and Substituent Effect. *J. Phys. Chem. C* **2014**, *118*, 6046−6051.
2. Yuan, C.; Wu, Q.; Li, Q.; Duan, Q.; Li, Y.; Wang, H-G. Nanoengineered Ultralight Organic Cathode Based on Aromatic Carbonyl Compound/Graphene Aerogel for Green Lithium and Sodium Ion Batteries. *ACS Sustain. Chem. Eng.* **2018**, *6*, 8392−8399.
3. Song, Z.; Zhan, H.; Zhou, Y-H. Polyimides: Promising Energy-Storage Materials. *Angew. Chem. Int. Ed.* **2010**, *49*, 8444–8448.
4. Pluczyk, S.; Higginbotham, H.; Data, P. Takeda, Y., Minakata, S. The impact of replacement of nitrogen with phosphorus atom in the pyromellitic diimides on their photophysical and electrochemical properties. *Electrochim. Acta* **2019**, *295*, 801–809.
5. Kim, D.J.; Je, S.H.; Sampath, S.; Choi, J.W.; Coskun, A. Effect of N-substitution in naphthalenediimides on the electrochemical performance of organic rechargeable batteries. *RSC Adv.* **2012**, *2*, 7968–7970.
6. Wang, D.; Huang, S.-P.; Wang, C.; Yue, Y. Zhang, Q-S. Computational Prediction for Oxidation and Reduction Potentials of Organic Molecules Used in Organic Light-Emitting Diodes. *Org. Electron.* **2019**, *64*, 216–222.
7. Shoaib, M.; Bibi, S.; Ullah, I.; Jamil, S.; Iqbal, J.; Alam, A.; Saeed, U.; Bai, F.Q. Theoretical Investigation of Perylene Diimide derivatives as Acceptors to Match with Benzodithiophene based Donors for Organic Photovoltaic Devices. *Z. Phys. Chem.* **2021**, *235*, 427–449.
8. Ji, L.-F.; Fan, J.-X.; Zhang, S.-F.; Ren, A-M. Theoretical investigations into the charge transfer properties of thiophene α-substituted naphthodithiophene diimides: Excellent n-channel and ambipolar organic semiconductors. *Phys.Chem. Chem. Phys.* **2017**, *19*, 13978–13993.
9. Frisch, M.J.; Trucks, G.W.; Schlegel, H.B.; Scuseria, G.E.; Robb, M.A.; Cheeseman, J.R.; Scalmani, G.; Barone, V.; Petersson, G.A.; Nakatsuji, H.; et al. *Gaussian 16, Revision B.01*; Gaussian, Inc.: Wallingford, CT, USA, 2016.

10. Wang, M.; Dong, X.; Escobar, I.C.; Cheng, Y-T. Lithium Ion Battery Electrodes Made Using Dimethyl Sulfoxide(DMSO) A Green Solvent. *ACS Sustain. Chem. Eng.* **2020**, *8*, 11046–11051.
11. Allouche, A.-R. Gabedit—A graphical user interface for computational chemistry softwares. *J. Comput. Chem.* **2011**, *32*, 174–182.
12. Evans, D.H. One-Electron and Two-Electron Transfers in Electrochemistry and Homogeneous Solution Reactions. *Chem. Rev.* **2008**, *108*, 2113–2144.
13. Gileadi, E. Simultaneous two-electron transfer in electrode kinetics. *J. Electroanal. Chem*. **2002**, *532*, 181–189.